Pattern formation in a granular medium excited by waves in a flume

Julie Lebunetel-Levaslot, Armelle Jarno-Druaux, François Marin

Journal of Physics: Conference Series **137** (2008) 012031 doi:10.1088/1742-6596/137/1/012031

Pattern formation in a granular medium excited by waves in a flume

Julie Lebunetel-Levaslot, Armelle Jarno-Druaux & François Marin

Laboratoire Ondes et Milieux Complexes FRE 3102 CNRS - 53, rue de Prony - BP 540 - 76058 Le Havre - FRANCE

julie.levaslot@univ-lehavre.fr, ajd@univ-lehavre.fr, francois.marin@univ-lehavre.fr

Abstract. This work deals with the dynamics of sand ripples which occur on a flat sandy sea bed excited with an oscillatory flow in a wave flume. The bathymetry of the bed is reported since the first stages of ripple formation with an optical technique. A statistical approach is developed to study the dynamical evolution of ripples. With an identical mobility number and different Reynolds number, two tests leading to 2D and 3D pattern formation are compared. Two stages are detected during ripple formation independently of pattern morphology. However, pattern tridimensionality can be detected with statistical tools. 2D and 3D equilibrium ripple geometric data are compared with the literature.

1. Introduction

Various ripple patterns are observed in shallow marine environments. Sometimes, sandy non-cohesive seabeds are covered with regular two-dimensional ripples, sometimes the patterns appear more complex and three-dimensional ripples can be observed.

When studying the ripples formation from an initial flat bed, two main classes of ripples are observed. First, rolling grain ripples appear at the very beginning of ripple formation. The transient nature of these small structures is experimentally demonstrated in different geometries (Faraci & Foti [1]; Rousseaux & *al.* [2]). This unstable state is followed by the vortex ripple state where ripples are due to the formation and shedding of organized vortices at the crests. Ripples are traditionally characterized by their mean length and height. However, even for 2D patterns, the spatial variability of ripples formed by a monochromatic gravity wave of high quality in a flume suggests that statistics on distributions of ripple geometric data can give further information on ripple patterns formation (Jarno-Druaux & *al.* [3]).

In the case of three-dimensional complex morphologies, theoretical studies have been performed in order to explain the formation mechanisms. Particularly concerning brick-pattern ripples, Hara & Mei [4] argue that the formation of such longitudinal structures is due to a hydrodynamic instability of the Görtler type. Indeed, this centrifugal instability is induced by the curved streamlines and the longitudinal vortices erode the ripples perpendicularly to their crest direction. Granular instability has been studied by Vittori & Blondeaux [5] and by Roos & Blondeaux [6]. They established, with a weakly nonlinear stability analysis of a flat cohesionless bottom subjected to an oscillatory flow, that the interactions between 2D and 3D bed perturbations can lead to brick-pattern ripple formation.

Three dimensional patterns are observed both in-situ and in laboratory but very few experimental studies have been conducted to measure and characterize 3D ripples until the recent work conducted

by O'Donoghue & *al.* [7]. It appears, during their full scale experiments, that the grain size is a prevailing factor for the formation of 3D pattern. Furthermore, they propose a formulation based on a modified Nielsen law [8] for 2D and 3D ripple heights and lengths at the equilibrium state. Three-dimensional ripple characteristics (height and length) are known to be smaller than those observed with 2D ripples, and this change has of course a great influence on sediment transport. However, the criteria of appearance of 3D ripples and their way of growth are still misunderstood and need further research.

Herein, a comparison between a 2D and a 3D pattern obtained with a same mobility number is reported. The equilibrium dominant geometric ripple lengths and heights for 2D and 3D patterns are compared with the literature.

2. Experimental set-up

2.1. Experimental facilities and test conditions

The experiments were carried out in a wave flume at LMPG, University of Le Havre. The wave channel has a 10m long, 0.5m high and 0.5m wide section. The movable bed is excited by a unidirectional oscillatory forcing flow. The tests were carried out with three natural sands with different grain-size distributions (d_{50} = *111* μ*m*, *163* μ*m*, *375* μ*m*, relative density: $s = 2.65$ and angle of repose: φ = 33 °). The *25 mm* depth of sandy bed is overlayed by a *27 cm* water layer. The experiments were carried out with several flow conditions for each type of sand. The flow conditions have been chosen such as the Reynolds number associated to the boundary layer, $R_\delta = \delta a \omega / \nu$, varies in the range $70 < R_\delta < 250$, where δ is the Stokes layer thickness, a is the fluid-orbital amplitude at the edge of the boundary layer, ω denotes the flow frequency and ν is the fluid kinematic viscosity. The mobility number ψ is defined as follow: $\psi = (a\omega)^2 / (s - 1)\, g\, d_{50}$ where d_{50} is the median grain size diameter, and varies between *3* and *38*. For each test, the first *6000* cycles of excitation are studied.

2.2. Experimental technique and processing

The measurement technique of ripple bathymetry is based on image acquisition fully detailed by Marin & Ezersky [9]. After a chosen number of excitation cycles, the wavemaker is stopped, a scan of the bed is performed and a bathymetry picture processed by the software LabView 6.1. The dimensions of the observed field are 6 m long and 35 cm width. The spatial resolution on both the horizontal and vertical directions is 0.5 mm per pixel. A specific signal processing is developed to get ripples geometric characteristics. Every line of the bathymetry picture is taken into account and the position of crests and troughs and thus the lengths and heights distributions are obtained applying a 1D-Hilbert transform on the signal and its "mirror". For each detected ripple, its length L, height H, steepness H / L, and mass M are calculated. Information of the whole pattern are then gathered. This leads to distribution function representation of ripple geometrical data, and thus statistics and probabilities calculations on the bed morphology are performed.

3. Results

3.1. Observation of ripple pattern formation

The tests begin from rest with a flat sandy bed. Ripples appear either uniformly over the test section or from nucleation sites according to the flow and sediments conditions. However, ripple patterns always formed uniformly over the test section for previous tests (Jarno-Druaux & *al.*, [3]) which were carried out with plastic powder (PolyVinyl Chloride; PVC) in the same wave flume as for present tests. Using PVC powder, a rolling grain ripple stage could be clearly characterized. In the present work performed with sand, the rolling of grains is observed but an organized rolling grain ripple pattern is not always detected partly due to its rapidity of conversion into vortex ripples.

In the particular case of flow and sand conditions that lead to 3D pattern, during the very beginning of excitation load, the sandy bed could be covered with different ripple patches which have not the

same geometric characteristics (height or length) and even not the same morphologies (2D or 3D), (figure 1).

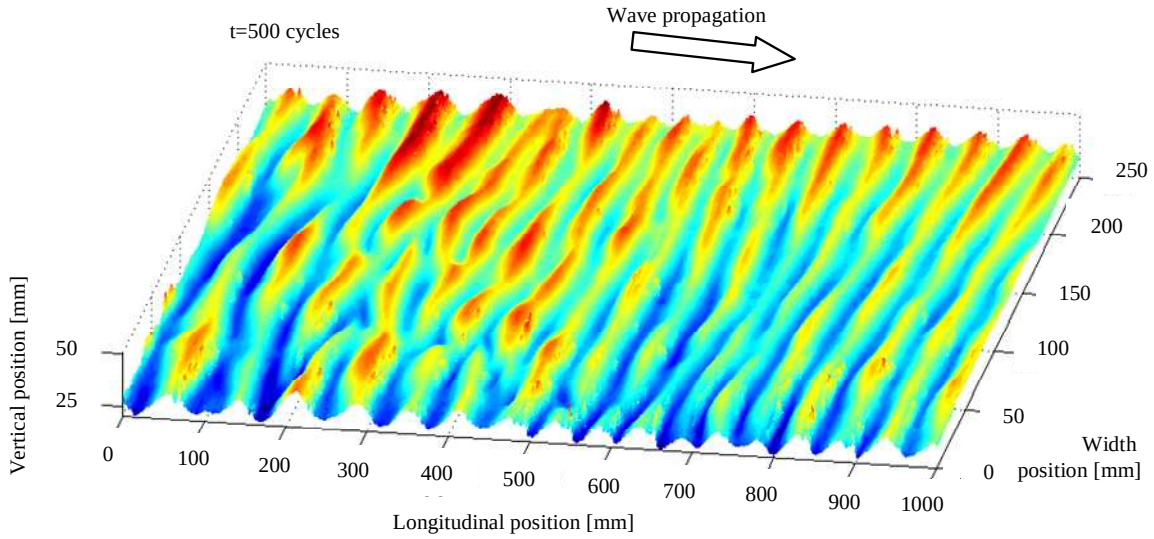

Figure 1. Bathymetry of a 1m long and 25cm width section of the bed at t=500 cycles (ψ=9 and R_δ=132).

3.2. The two stages in pattern evolution

In this section are compared two tests for which the mobility number is the same ($\psi = 9$), but with different Reynolds number R_δ. A change of the value of R_δ for a given value of ψ is obtained varying the wave conditions (an increase of the wave period or of the wave height leads to higher Reynolds numbers). The main difference between the patterns observed in those experiments is that one of them leads to a 2D ripple geometry (for $R_\delta = 98$) and the other leads to a 3D morphology (for $R_\delta = 132$). Similarities are first observed concerning the global trend of ripple geometrical characteristics evolution. Indeed, two main stages are detected. The first one is a rapid growth stage and has a typical duration of 700 cycles. Ripples characteristics grow, at a local scale, until they reach almost 90% of their equilibrium value (figure 2a). At the same time, the adimensioned standard deviation Σ (ratio between the standard deviation and dominant value of the studied repartition) strongly decreases and reaches its minimum at the end of this first stage (figure 2b), leading to the most regular pattern during the ripples formation. Afterwards, the growth rate of ripple data is weak. Dominant values are kept quite constant but distributions still undergo changes that are captured by the standard variation. In particular, we notice an increase of Σ at the very beginning of the second stage suggesting that the pattern slightly 'dilate' while organizing at the global flume scale.

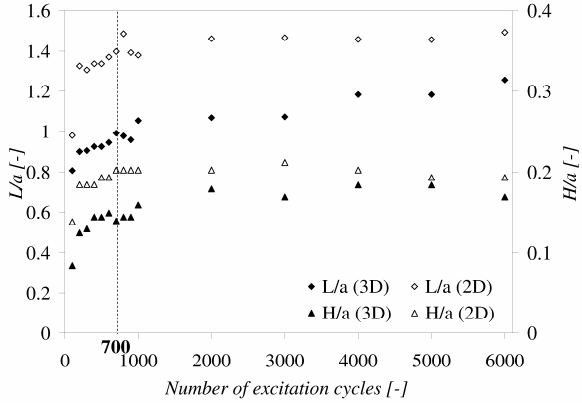

Figure 2a. Evolution with time of *L/a* and *H/a* for 2D and 3D patterns($\psi = 9$, $R_{\delta(2D)} = 98$, $R_{\delta(3D)} = 132$).

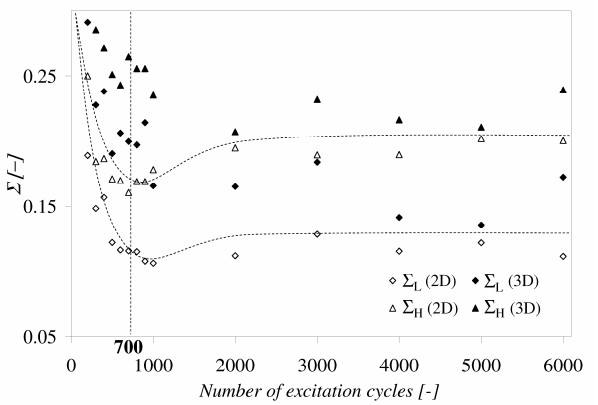

Figure 2b. Evolution with time of Σ_L and Σ_H for 2D and 3D patterns($\psi = 9$, $R_{\delta(2D)} = 98$, $R_{\delta(3D)} = 132$).

Furthermore, the values of Σ are much higher for the 3D case than for the 2D. This result suggests that despite an evident uniformization of the pattern at the end of the first stage, the diversity in ripple length and height for the 3D rippled bed remains considerable.

3.3. Equilibrium state

Figure 3 reports our results for the dominant values of ripple height and length at the equilibrium state; the values of the ranges of the hydrodynamic and sedimentary parameters are given in section 2.1. Nielsen [8] and O'Donoghue & *al.* [7] formulae are also plotted on this figure. O'Donoghue & *al.* introduced two modified Nielsen formulae for 3D and 2D ripple patterns. Let us note that our experiments are performed with small values of ψ and R_δ, whereas O'Donoghue & *al.* focused their work on experimental conditions leading to higher values of ψ and R_δ.

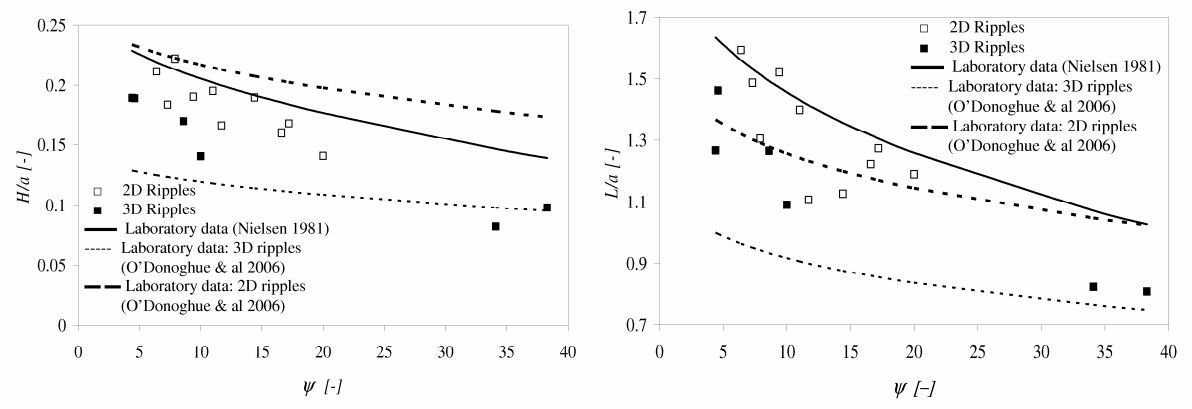

Figure 3. Equilibrium values of *H/a* and *L/a* for every test and comparison with experimental laws.

As expected, the ripples geometric dimensions are smaller in the case of 3D patterns than in the case of 2D patterns. The prediction of O'Donoghue & *al.* for 3D ripples gives a good correspondence with our results for the present high values of ψ. However, a strong increase of the equilibrium values of ripple heights and lengths is clearly shown at smaller values of ψ, which is not predicted by O'Donoghue & *al.* law. Moreover, it is observed that, for the tested parameters ranges, ripple length at the equilibrium depends on two control parameters: the mobility number and the Reynolds number associated to the flow. For a given value of ψ, the ripple length decreases for increasing values of R_δ, with a stronger influence of the Reynolds number at low values of ψ. Concerning the appearance of 2D or 3D ripple patterns, it clearly depends on both flow and sediment properties. However, no critical value of R_δ and ψ could be determined with the present tests.

4. Conclusions

This study considers the formation of 2D and 3D sand ripples in a wave flume. Two different stages of ripple pattern formation are identified by a statistical analysis of ripple heights and lengths. The first one corresponds to a rapid growth stage at a local scale and the second one traduces a global organization of the pattern. These observations are made for 2D and 3D patterns even if the 2D cases highlight more clearly the behaviors of the pattern. Studying the pattern evolution since the first stages of ripple formation, it is observed that the pattern geometry (2D/3D) is not necessary the same at the beginning of the test and at its end. In some cases, pattern is first 2D and, after the rapid growth stage, it turns to 3D pattern, coming with a global reorganization of the pattern (traduced by an increase in standard deviation of geometrical data). For a given mobility number, 3D ripples are obtained with higher values of Reynolds number than for 2D ripples. The dimensions of 3D ripples at the equilibrium state are smaller than in the 2D cases, at fixed mobility number. Considering 2D and 3D

patterns, equilibrium values of lengths depend not only on the mobility number, but also significantly on the Reynolds number at low mobility number. Finally, the present results suggest that an exclusive estimation of dominant geometric parameters looks insufficient to capture the main features of 3D patterns.

References

[1] Faraci C and Foti E 2001 *Physics of Fluids* **13** issue 6
[2] Rousseaux G, Stegner A and Wesfreid J E 2004 *Physical Review E* **69**
[3] Jarno-Druaux A, Brossard G and Marin F 2004 *EJM B/Fluids* **23** 695–708
[4] Hara T and Mei C C 1990 *Journal of Fluid Mechanics* **217** 1–32
[5] Vittori G and Blondeaux P 1992 *Journal of Fluid Mechanics* **239** 23–45
[6] Roos P C and Blondeaux P 2001 *Journal of Fluid Mechanics* **447** 227–46
[7] O'Donoghue T, Doucette J S, Van der Werf J J and Ribberink J S 2006 *Coastal Engineering* **53** 997–1012
[8] Nielsen P 1981 *Journal of Geophysical Research* **86**(7) 6467–72
[9] Marin F and Ezersky A B 2007 *EJM B/Fluids*, doi: 10.1016/j.euromechflu.2007.05.003